Approach to Gaussian stochastic behavior for systems driven by deterministic chaotic forces

Angela Hilgers[1,*] and Christian Beck[2]
[1]Institut für Theoretische Physik, RWTH Aachen, Templergraben 55, 52056 Aachen, Germany
[2]School of Mathematical Sciences, Queen Mary and Westfield College, University of London, Mile End Road, London E1 4NS, England

(Received 17 February 1999)

We consider skew-product dynamical systems that describe the stroboscopic dynamics of a damped particle subjected to a chaotic kick force. In a suitable scaling limit the dynamics converges to the Ornstein-Uhlenbeck process. We investigate the deterministic chaotic corrections in the vicinity of this Gaussian limit case for various examples of chaotic forces. We present numerical evidence that, for certain classes of chaotic forces, the deterministic chaotic corrections of the invariant density are universal. We provide analytical results for forces generated by Tchebyscheff maps and sketch a renormalization group theory in the space of probability densities. [S1063-651X(99)11610-6]

PACS number(s): 05.45.−a

I. INTRODUCTION

An interesting problem in statistical physics is the connection between random behavior of Brownian motion type on a mesoscopic scale and an underlying deterministic dynamics on a microscopic scale [1–11]. Dynamical systems of Langevin type (or, in general, of skew-product form) can be regarded as suitable models for these types of problems [12–22]. In the simplest case they describe the stroboscopic dynamics of a particle that moves in damping medium under chaotic kicks, which evolve in a deterministic way on a fast time scale. The force on the fast time scale is not Gaussian white noise (as it is for the Langevin equation) but a more complicated, *a priori* arbitrary chaotic process, generated by a deterministic evolution rule. For the case of a linear damping, one obtains maps of Kaplan-Yorke type [23]. Many aspects of such dynamics have been investigated, dealing with ergodic and mixing properties [15,17,18,20], the dimension of the attractor [16,21,23], higher-order correlation functions [19], invariant densities [15,24], and many other properties. Generalizing the concept to higher dimensions, physical applications have been pointed out for turbulence [25–27] and quantum-field theories [28,29].

For the maps of skew-product form considered here, under certain assumptions concerning the mixing properties of the chaotic driving force, it has been proven that the complicated chaotic dynamics reduces to a Langevin process in an appropriate scaling limit (regarding the initial values as random variables). The proof is based on functional central limit theorems for weakly dependent events [13,30]. For example, the convergence to the Langevin process has been proved rigorously for kick forces generated by Tchebyscheff maps or any other map conjugated to a Bernoulli shift, as well as for other maps such as the continued fraction map. Many interesting results on central-limit theorems for dynamical systems are well known in the mathematical literature [30–44].

*Present address: Center for Turbulence Research, Bldg. 500, Stanford University, Stanford, CA 94305-3030.

In this paper we systematically investigate various types of chaotic kick forces where it is known that the system approaches a Langevin process (the Ornstein-Uhlenbeck process) in the scaling limit. We are interested in the deterministic chaotic corrections in the vicinity of this limit case. We will investigate the deviations of the invariant density from the Gaussian density for many examples of chaotic driving forces. We will provide numerical evidence that often the approach to the Gaussian density takes place via scaling behavior of the leading order correction with the time scale parameter. Moreover, we will provide numerical evidence for universal behavior. That is to say, for certain classes of chaotic forces, one always finds the same deterministic chaotic corrections of the invariant density in the vicinity of the Gaussian limit case. We will present analytical results obtained for Tchebyscheff polynomials where the dynamics can be understood completely. Finally, we will sketch a renormalization-group approach to this problem.

II. NUMERICAL INVESTIGATION OF UNIVERSALITY PROPERTIES

We investigate dynamical systems of the skew-product form

$$x_{n+1}=T(x_n),$$
$$u_{n+1}=\lambda u_n+\sqrt{\tau}x_n,\quad \lambda=e^{-\tau}. \tag{1}$$

T is some chaotic mapping and τ is a small time scale parameter. The above kind of map is called a map of linear Langevin type [12] since it is related to the linear Langevin equation describing dynamical Brownian motion [45]. u_n corresponds to the stroboscopic velocity of a particle in a viscous medium subjected to a chaotic kick force. Integrating the equation of motion

$$\dot{u}=-\gamma u+\sqrt{\tau}\sum_{n=1}^{\infty} x_{n-1}\delta(t-n\tau), \tag{2}$$

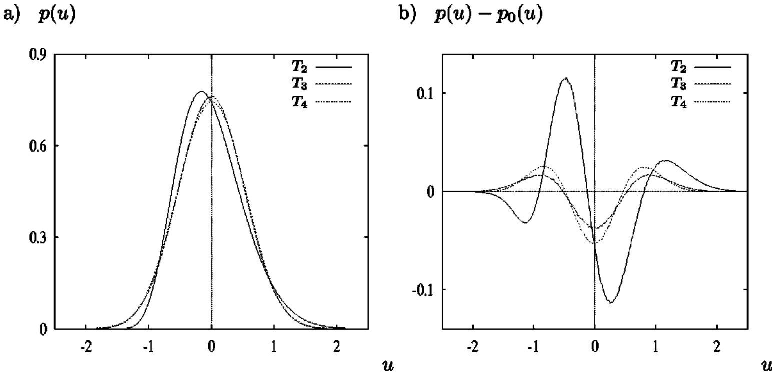

FIG. 1. (a) Invariant density $p(u)$, and (b) deviation of $p(u)$ from the Gaussian $p_0(u)$ for the second, third, and fourth Tchebyscheff polynomial; $\tau=0.1$.

one obtains recurrence relation (1) for the velocity u_n immediately after the kick. For convenience, we have chosen $\gamma=1$ and rescaled the kick strengths by the factor $\sqrt{\tau}$.

We characterize the process generated by map (1) by the marginal invariant density $p(u)$ of the u variable. The dynamics generated by various maps T such as the Tchebyscheff polynomials, the tent and the continued fraction map, the map $T(x)=1-2x^4$, the logistic map, and the binary shift map will be analyzed. For all examples of maps investigated in this paper, the numerical simulation of Eq. (1) confirms that the marginal invariant density converges to a Gaussian distribution $p_0(u)$ in the limit $\tau\to 0$. For certain maps T, this can actually be proved rigorously. If the map T possesses the so-called φ mixing property (a slightly stronger condition than the ordinary mixing property) it can be shown that the solution $u(t)$ of Eq. (2) converges to the Ornstein-Uhlenbeck process in the limit $\tau\to 0$, $t=n\tau$ finite, regarding the initial values x_0 as random variables [13,30]. Hence in this limit there is equivalence between Eq. (1) and the Langevin equation, and the rescaled deterministic chaotic kick force reduces to Gaussian white noise. On the other hand, for a finite time scale τ, which is inherent in any physical system, there are deviations of the invariant density $p(u)$ from the Gaussian $p_0(u)$. These deviations depend on the map T.

In order to understand these deviations, we have performed an intensive numerical study for various standard examples of maps T. For each choice of T we have performed 10^8 iteration steps of Eq. (1) and have calculated histograms of the u variable. We have repeated the calculation for several values of the time scale parameter τ. For some maps T the standard deviation of the Gaussian $p_0(u)$ approached in the limit of vanishing τ is known analytically [13]. In this case the deviations from the Gaussian $p(u)-p_0(u)$ can be evaluated immediately. If the standard deviation is not known, we have determined it numerically from a simulation with a very small value of τ.

A. The Tchebyscheff polynomials

We start with the case in which the map T in Eq. (1) is a Tchebyscheff polynomial T_N of order N. It has been shown in [19] that for these polynomials the number of nonvanishing higher-order correlations is smaller than for any other deterministic map semiconjugated to a shift. Therefore, the T_N have strongest random properties and the dynamics is, in a sense, closer to Gaussian white noise than that generated by any other smooth chaotic map. Since the Tchebyscheff polynomials are φ mixing, the process generated by the variable u_n in Eq. (1) is known to converge to the Ornstein-Uhlenbeck process in the limit $\tau\to 0$. For all N, in this limit case the invariant density is given by the Gaussian

$$p_0(u)=\sqrt{\frac{2}{\pi}}e^{-2u^2}. \tag{3}$$

We consider the polynomials

$$\begin{aligned} T_2(x)&=2x^2-1,\\ T_3(x)&=4x^3-3x,\\ T_4(x)&=8x^4-8x^2+1,\\ T_5(x)&=16x^5-20x^3+5x,\\ T_6(x)&=32x^6-48x^4+18x^2-1, \end{aligned} \tag{4}$$

and initial values $x_0\in[-1,1]$. It is possible to obtain an analytic expression for the probability density $p(u)$ for small but finite τ by considering a perturbative expansion in the time constant τ. The corrections to the Gaussian can be determined either from the Perron Frobenius equation [24] or by an investigation of higher-order correlations and subsequent Fourier transformation [19]. The calculation has so far been explicitly carried out for the map T_2, yielding [19,24]

$$p(u)=[1+\tau^{1/2}c(-2u+\tfrac{8}{3}u^3)]p_0(u)+O(\tau), \tag{5}$$

where $c=1$ for the Tchebyscheff map T_2 and $c=-1$ for the Ulam map $-T_2$. Note that the first correction term of order $\tau^{1/2}$ consists of an odd polynomial multiplied by the Gaussian $p_0(u)$.

Figure 1(a) shows numerical results for the invariant density $p(u)$ obtained for the second, third, and fourth Tchebyscheff polynomial. The plots were obtained by iterating Eq. (1) for the parameter value $\tau=0.1$ and using the histogram method. While the probability density for $T_2(x)$ shows a clear asymmetry, $p(u)$ is symmetric or almost symmetric for the Tchebyscheff polynomials of higher order. This is confirmed by Fig. 1(b), which shows the deviations from the Gaussian $p(u)-p_0(u)$. In Sec. III we will outline how the invariant density can be analytically calculated for the Tchebyscheff polynomials of arbitrary order $N\geqslant 2$.

It has been proved in [12] that $p(u)$ is symmetric if $T(x)$ is an odd function and if at the same time the invariant density $\rho(x)$ of T is an even function of x. Since for all Tchebyscheff maps T_N the invariant density

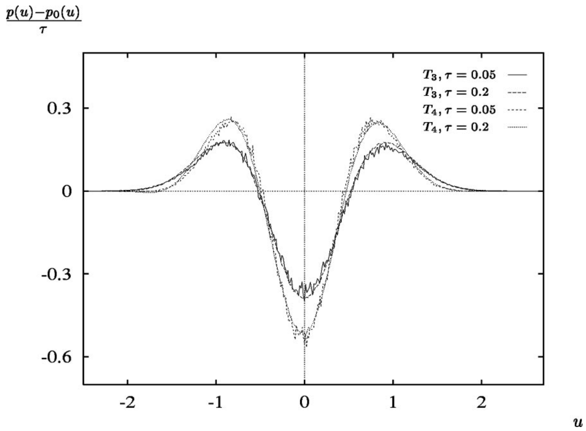

FIG. 2. Scaling of the deviations from the Gaussian $p(u)-p_0(u)$ for the third and fourth Tchebyscheff polynomial; $\tau=0.05$ and $\tau=0.2$.

$$\rho(x)=\frac{1}{\pi\sqrt{1-x^2}} \tag{6}$$

is an even function, the symmetry of $p(u)$ is thus understood for all Tchebyscheff maps with odd N. On the other hand, there is no simple explanation for the symmetry of $p(u)$ generated by T_4 and T_6. We will come back to this in Sec. III.

Figure 2 shows the deviations from the Gaussian for the third and fourth Tchebyscheff polynomials, calculated for two different values of the time constant $\tau=0.05$ and $\tau=0.2$. The smaller the deviations from the Gaussian, the more difficult it is to calculate them with a small statistical error. We have divided the deviation $p(u)-p_0(u)$ by τ in order to analyze the scaling behavior with τ. Since the curves in Fig. 2 calculated for different τ do not differ significantly, there is numerical evidence that the first correction to the Gaussian is of order τ. This stands in clear contrast to T_2, where it is of order $\tau^{1/2}$. Generally, no corrections of order $\tau^{1/2}$ are observed for arbitrary Tchebyscheff polynomials of order $N\geqslant 3$.

Further increasing the index N, one notices that for the Tchebyscheff polynomials of order $N\geqslant 4$ the invariant densities $p(u)$, as calculated by the histogram method, coincide for all N within the statistical error. This is shown in Fig. 3. We will explain this fact in Sec. III.

B. The tent and continued fraction map

The tent map

$$T(x)=1-2|x|, \quad x\in[-1,1] \tag{7}$$

is semiconjugated to the Bernoulli shift and hence is φ mixing. It is an even function of x and it has an even invariant density $\rho(x)=\frac{1}{2}$ on $[-1,1]$. Though the tent map is topologically conjugated to the second Tchebyscheff polynomial T_2, the entire two-dimensional map (1) is not, and hence a different dynamics arises. When iterating Eq. (7), noise of small amplitude is added to the iterates x_n in order to avoid numerical errors that occur when the trajectory comes close to the fixed point $x=-1$.

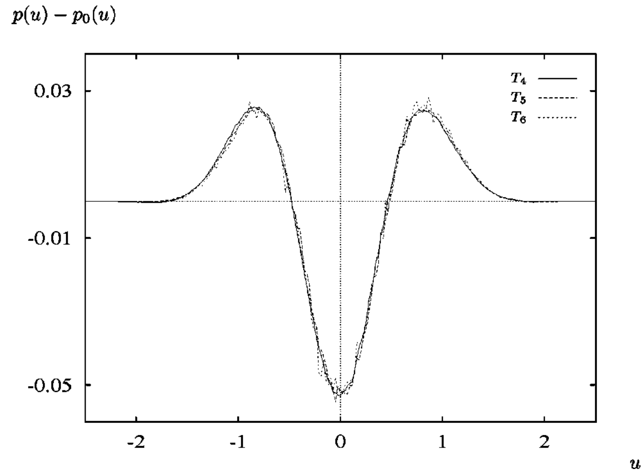

FIG. 3. Deviations of $p(u)$ from the Gaussian $p_0(u)$ for the Tchebyscheff polynomials T_4, T_5, and T_6; $\tau=0.1$.

The continued fraction map

$$T(x)=\frac{1}{x}-\lfloor\frac{1}{x}\rfloor, \quad x\in(0,1] \tag{8}$$

is also φ mixing. However, it is not conjugated to a shift. Neither map (8) nor its invariant density

$$\rho(x)=\frac{1}{(1+x)\ln 2} \tag{9}$$

have simple symmetry properties. When iterating map (1) the mean value $\langle x\rangle=1/\ln 2-1$ is subtracted from x_n in order to obtain a kick force with average 0.

Again we have numerically calculated the marginal invariant densities $p(u)$ for different values of the time constant τ and compared the respective deviations from the Gaussian distribution. Both maps yield an asymmetric density $p(u)$, just like the Tchebyscheff polynomial of second order. Figure 4 shows the deviations for different values of τ. In the case of the tent map the functions $[p(u)-p_0(u)]/\sqrt{\tau}$ agree well for different values of the time constant. The convergence of the invariant density to a Gaussian for $\tau\rightarrow 0$ is slower for the continued fraction map; higher-order terms play a more significant role. For both the tent and the continued fraction map the deviations from a Gaussian show scaling behavior with $\sqrt{\tau}$ for sufficiently small τ.

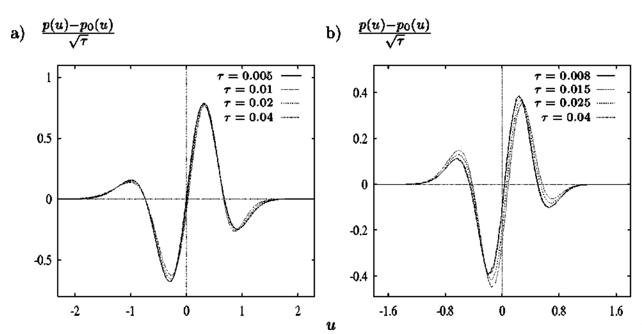

FIG. 4. Scaling of the deviations $p(u)-p_0(u)$ for (a) the tent and (b) the continued fraction map.

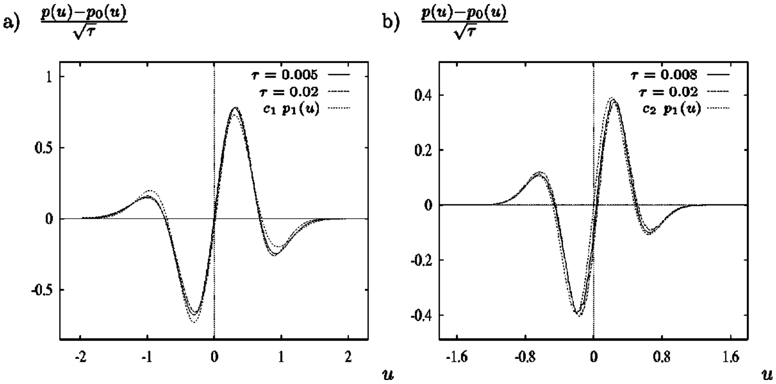

FIG. 5. Scaling properties of (a) the tent map, $\tau=0.005$, and $\tau=0.02$ and (b) the continued fraction map, $\tau=0.008$, and $\tau=0.02$; comparison with the function $c_1p_1(u)$ and $c_2p_1(u)$ with $c_1=1.62$ and $c_2=0.59$.

In Fig. 5 we compare the deviations from the respective Gaussian for the tent and the continued fraction map with those of the Ulam map. For this purpose we scaled the probability distributions such that the standard deviation takes the value $\sigma=1/2$ for all $p(u)$. There is numerical evidence that for both the tent and the continued fraction map there is convergence of $[p(u)-p_0(u)]/\sqrt{\tau}$ to $cp_1(u)$, with

$$p_1(u)=(2u-\tfrac{8}{3}u^3)p_0(u) \qquad (10)$$

being the analytical result obtained for the Ulam map. The limits obtained for all three mappings differ by the factor c only. Whereas $c=1$ for the Ulam map, we have $c=1.62$ for the tent map and $c=0.59$ for the continued fraction map. It can, therefore, be concluded that the first corrections to the Gaussian are given by expression (10) and that this expression has universal significance, being of relevance for several different maps.

C. The map $T(x)=1-2x^4$

For the map

$$T(x_n)=1-2x^4, \quad x\in[-1,1] \qquad (11)$$

the mixing properties are not known. The simulation has shown that large numerical errors occur when the trajectory reaches the vicinity of the fixed points. Therefore, a precise calculation of the invariant density $p(u)$ is difficult. Nevertheless, we have observed that the invariant density $p(u)$ converges to a Gaussian in the limit of a vanishing time constant. The deviations from the Gaussian are asymmetric and very close to those observed for the Ulam map. They show scaling with $\sqrt{\tau}$.

D. The logistic map

The dynamics of the logistic map

$$T(x)=1-\mu x^2, \quad x\in[-1,1] \quad \mu\in[0,2] \qquad (12)$$

is well known to depend on the value of the control parameter μ in a nontrivial way. For $\mu>\mu_\infty=1.401\,155\,189$ the motion is chaotic apart from the windows, where again stable periodic motion exists.

We have investigated the dynamics for values $\mu\in[1.8,2.0]$ that do not correspond to stable periodic motion. Apart from the value $\mu=2$, which corresponds to the Ulam map, and apart from special parameter values such as the Misiurewicz points, the mixing properties are not analytically known. For $\mu<2$ we have calculated the marginal invariant density $p(u)$ numerically. We again have subtracted the mean value $\langle x\rangle$ from x_n in Eq. (1). The invariant density $p(u)$ converges to a Gaussian with a different variance for each value of μ. It depends on the control parameter in a complicated fractal way (Fig. 6).

Figure 7 shows the deviations from the Gaussian for $\tau=0.04$ and $\tau=0.08$ and for six examples of the control parameter. The first figure once again shows the antisymmetric first-order term and the scaling with $\sqrt{\tau}$ observed for $\mu=2$. Deviations from antisymmetry are just due to the next perturbative term of order τ. When μ is decreased, the asymmetry of $p(u)$ becomes smaller. Even when μ is only slightly smaller than 2, the distribution has lost its scaling behavior with $\sqrt{\tau}$. For $1.999\geqslant\mu>1.95$ the deviations from the Gaussian are similar to those observed for the Tchebyscheff polynomials of order $N\geqslant3$ and the distributions scale approximately with τ. Three examples for this range are shown in Figs. 7(b)–7(d). While for $\mu=1.99$ and $\mu=1.96$ the functions $[p(u)-p_0(u)]/\tau$ are quite similar for different τ, deviations from this simple scaling behavior appear for $\mu=1.97$. A distinguished parameter value for which we have observed both exact scaling with τ and a symmetric deviation $p(u)-p_0(u)$ is $\mu=1.96$. For $\mu<1.94$ the distributions are different from those observed for the Tchebyscheff polynomials of higher-order. They are asymmetric and no simple scaling with a power of τ seems to exist. For some values

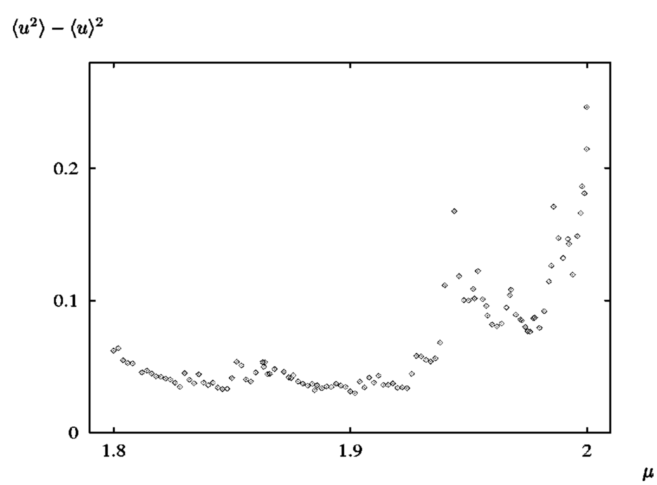

FIG. 6. Variance of $p(u)$ as a function of the control parameter μ; $\tau=0.002$.

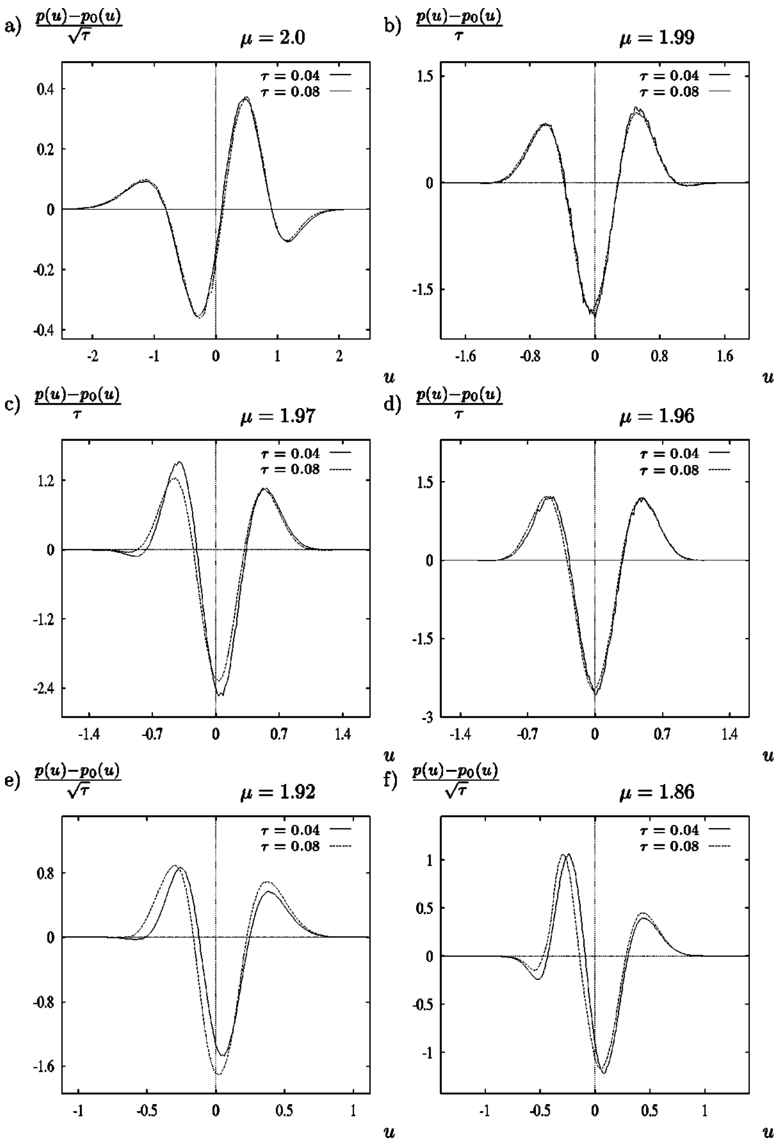

FIG. 7. Deviations from the Gaussian for the logistic map with (a) $\mu=2.0$, (b) $\mu=1.99$, (c) $\mu=1.97$, (d) $\mu=1.96$, (e) $\mu=1.92$, and (f) $\mu=1.86$; $\tau=0.04$ and 0.08.

$\mu<1.9$ there are invariant densities $p(u)$ for which the deviations of the Gaussian are antisymmetric or almost antisymmetric. Figure 7(f) indicates that for $\mu=1.86$ scaling with $\sqrt{\tau}$ appears again. The deviations from the Gaussian are antisymmetric (apart from higher-order terms), but this time the asymmetry has the opposite sign compared to the Ulam map in Fig. 7(a). Asymmetric distributions and scaling with $\sqrt{\tau}$ are typically observed in the vicinity of the windows.

Figure 8 confirms that for $\mu=1.96$ and $\mu=1.86$ the deviations correspond to those of the second and fourth Tchebyscheff polynomials (up to a multiplicative constant). This again indicates universality, i.e., the Tchebyscheff deviations from the Gaussian are relevant for other maps as well.

E. The binary shift map

The binary shift map is given by

$$T(x)=2x-\lfloor 2x\rfloor, \quad x_n\in[0,1) \tag{13}$$

where $\lfloor 2x\rfloor$ denotes the integer part of $2x$. Since a direct simulation of Eq. (13) yields problems with round-off errors, we have calculated the binary representation of x_n in every iteration step. x_{n+1} is then calculated by performing a shift of symbols and replacing the last digit randomly by 0 or 1. Since the average $\langle x_n\rangle=\frac{1}{2}$ does not vanish it is subtracted in Eq. (1).

The binary shift map is φ mixing. $T(x)$ is an odd function with respect to $x=\frac{1}{2}$ and its invariant density $\rho(x)=1$ is symmetric around $x=\frac{1}{2}$. Therefore, the invariant density

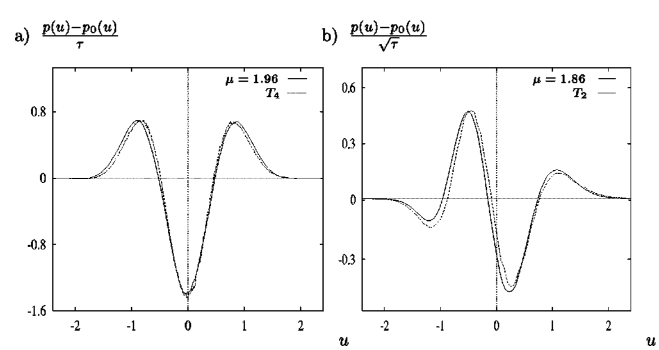

FIG. 8. Deviations from the Gaussian for the logistic map with (a) $\mu=1.96$ and (b) $\mu=1.86$, compared to those of the Tchebyscheff polynomials T_4 and T_2; (a) $\tau=0.1$, and (b) $\tau=0.02$.

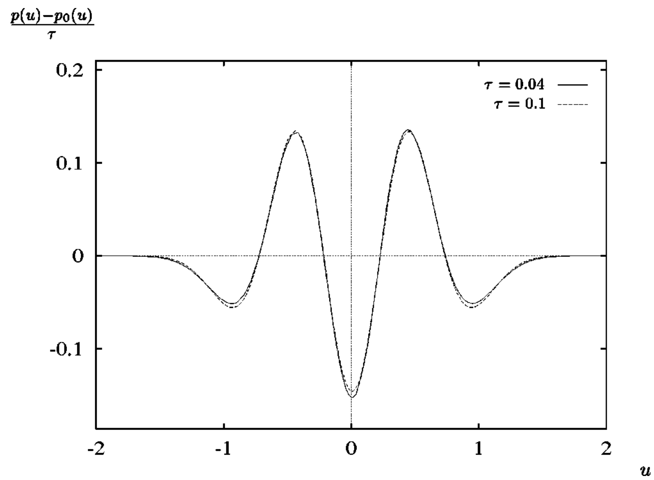

FIG. 9. Scaling of the deviations $p(u)-p_0(u)$ for the binary shift map; $\tau=0.04$ and $\tau=0.1$.

$p(u)$ is symmetric [12]. Figure 9 shows the deviations from the Gaussian that have been calculated with Eq. (1). Again the deviations have been divided by τ in order to show scaling with τ. The functions calculated for $\tau=0.04$ and $\tau=0.1$ are very similar, thus indicating that the lowest-order correction to the Gaussian scales with τ. For the binary shift map the shape of the deviation from the Gaussian is different from that calculated for the Tchebyscheff polynomials of any order. It spans up another universality class.

F. Random numbers

We have also investigated which form the invariant density takes on if the x_n are not generated by a deterministic chaotic map but chosen as independent random numbers. We have used equally distributed random numbers in $[-1,1)$ with invariant density $\rho(x)=\frac{1}{2}$. Again, convergence to a Gaussian is observed in the limit $\tau\rightarrow 0$. This, of course, is a consequence of the ordinary central-limit theorem for independent random variables. Figure 10 shows that for the dynamics generated by random numbers the deviations from the Gaussian scale with τ. In fact, the deviations are purely produced by the discreteness of dynamics (1), rather than by nontrivial higher-order correlations, as for chaotic maps. Nevertheless, apart from a multiplicative factor, the deviations for independent random variables are in very good agreement with those of the Tchebyscheff polynomials of fourth and higher order. Indeed, for those maps the graph-theoretical method of [19] shows that the $O(\tau)$ corrections coincide with those of independent random variables.

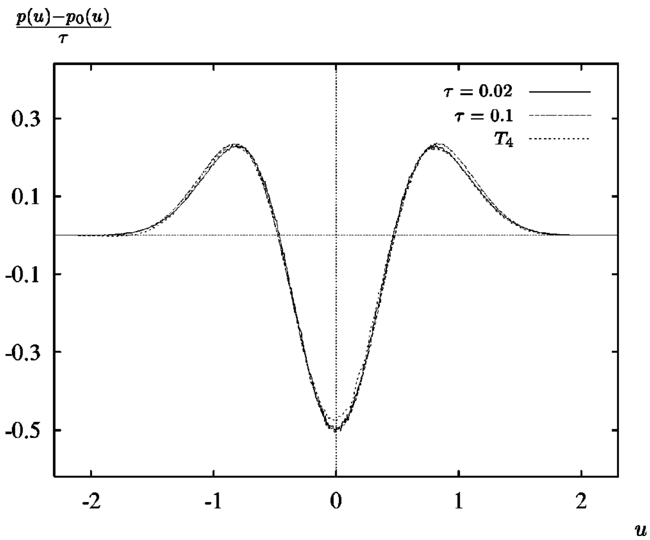

FIG. 10. Scaling of the deviations from the Gaussian for independent random numbers in $[-1,1)$, $\tau=0.02$, and $\tau=0.1$; comparison with the fourth Tchebyscheff polynomial for $\tau=0.1$.

G. Discussion

The symmetry and scaling properties of the maps analyzed in this paper are summarized in Table I. For the maps that are known to be φ mixing, the deviations from the Gaussian scale with either τ or $\tau^{1/2}$. For all maps considered here that are antisymmetric and that have a symmetric invariant density $\rho(x)$, the corrections to the Gaussian scale with τ. If the symmetry properties are different from this, both kinds of scaling are possible. Scaling with τ or $\tau^{1/2}$ has also been observed for maps that are not known to be φ mixing. There seem to exist various shapes of the deviations in the case of scaling with τ. On the other hand, if the first correction term to the Gaussian is of order $\sqrt{\tau}$, then this term appears to be always the same function, apart from a nonuniversal prefactor. The deviations generated by the Ulam map, tent map, continued fraction map, logistic map with, e.g., $\mu=1.86$ and the map $T(x)=1-2x^4$ all coincide in the limit of small values of τ. It can thus be concluded that these maps are members of one universality class. The invariant density $p(u)$ is described by Eq. (5). On the other hand, the Tchebyscheff polynomials of fourth and higher order and the logistic map for special values of the control parameter lead

TABLE I. Characteristic properties of some chaotic maps.

Map	φ mixing	T antisymmetric	ρ symmetric	$\lim_{\tau\rightarrow 0}\sigma$	Scaling
$T_3(x), T_5(x)$	yes	yes	yes	0.5	τ
$T_4(x), T_6(x)$	yes	no	yes	0.5	τ
Binary shift map	yes	yes	yes	$1/\sqrt{6}$	τ
$T_2(x)$	yes	no	yes	0.5	$\tau^{1/2}$
Tent map	yes	no	yes	$1/\sqrt{8}$	$\tau^{1/2}$
Continued fraction map	yes	no	no	0.277	$\tau^{1/2}$
$T(x)=1-2x^4$		no	no	0.615	$\tau^{1/2}$
Logistic map, some μ		no	no	varies	$\tau, \sqrt{\tau}$

to scaling with τ, spanning up another universality class. The deviations generated by all these maps agree with those observed for independent random numbers. The corresponding correction of order τ is not a consequence of the chaotic properties, but merely of the discreteness of map (1). Different corrections of order τ have been found for the binary shift map and for the Tchebyscheff polynomial of third-order. Apparently, for maps that generate scaling behavior with τ, there exist several paths to approach the Gaussian limit. For those that scale with $\sqrt{\tau}$, however, we have only observed one such path.

III. PERTURBATION THEORY

In this section we present analytical results for the invariant probability density $p(u)$ of process (1) for the case in which the map T is a Tchebyscheff polynomial of arbitrary order N. We will only give an outline of the procedure here. Details of the calculation will be presented elsewhere.

The approach is based on a perturbative calculation of higher-order correlations for small values of the time constant τ. The r-point correlation of the x dynamics is

$$E(x_{j_1}x_{j_2}\dots x_{j_r}) := \int_{-1}^{1} dx_0 \rho(x_0) T^{j_1}(x_0) T^{j_2}(x_0)\dots T^{j_r}(x_0),$$

where ρ is the natural invariant density of T. For the special case in which T is the Tchebyscheff polynomial of second order, the r-point correlations have been investigated in detail in [19]. It has been shown that the nonvanishing correlations correspond to a set of graphs. These graphs consist of incomplete double binary forests with r leaves.

Let us now consider the r-point correlation functions $E(u_{n_1},\dots,u_{n_r})$. If we choose the initial condition $u_0=0$ in Eq. (1), we obtain

$$u_n = \tau^{\frac{1}{2}} \sum_{j=0}^{n-1} c(j) x_j \tag{14}$$

with $c(j)=\lambda^{n-j-1}$. The r-point correlations for u_n thus are a superposition of the $E(x_{j_1}\cdots x_{j_r})$,

$$E(u_{n_1}\cdots u_{n_r}) = \tau^{\frac{r}{2}} \sum_{j_1=0}^{n_1-1} \dots \times \sum_{j_r=0}^{n_r-1} c(j_1)\dots c(j_r) E(x_{j_1}\dots x_{j_r}).$$

This allows us to obtain an expression for the correlations $E(u_{n_1},\dots,u_{n_r})$ and the moments $E(u_n^r)$ using the graphs of [19]. The fact that each type of graph corresponds to a certain power of $\sqrt{\tau}$ allows for a perturbative calculation of the correlation functions.

Using the characteristic function

$$G(k) := E(e^{iku_n}) = \sum_{r=0}^{\infty} \frac{(ik)^r}{r!} E(u_n^r), \tag{15}$$

we obtain the invariant density by Fourier transformation of $G(k)$ in the limit $n\to\infty$,

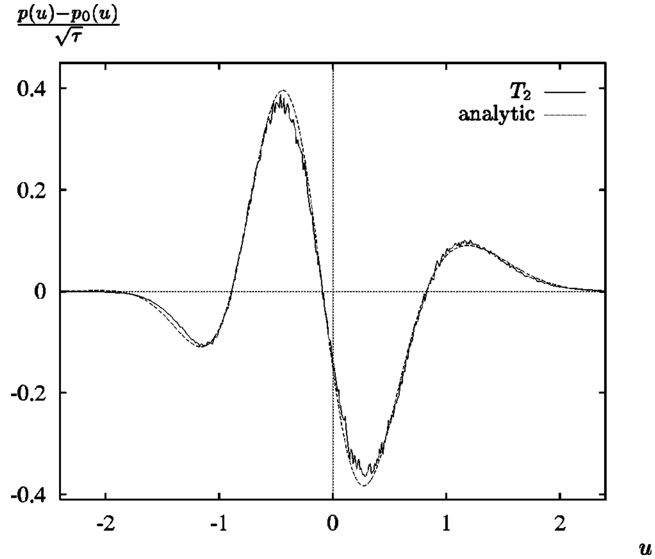

FIG. 11. Comparison of perturbative result (17) with the numerical result for T_2; $\tau=0.06$.

$$p(u) = \frac{1}{2\pi} \int_{-\infty}^{+\infty} dk G(k) e^{-iku}. \tag{16}$$

We have extended the approach presented in [19] to Tchebyscheff polynomials of arbitrary order. The calculation is lengthy but straightforward. The final perturbative result for the invariant density, including terms up to order τ is for the Tchebyscheff polynomial of second order [19,24],

$$p^{N=2}(u) = \sqrt{\frac{2}{\pi}}[1+\tau^{\frac{1}{2}}(-2u+\tfrac{8}{3}u^3) + \tau(\tfrac{32}{9}u^6 - \tfrac{31}{3}u^4 + \tfrac{15}{2}u^2 - \tfrac{37}{48})]e^{-2u^2} + O(\tau^{3/2}); \tag{17}$$

for the polynomial of third order,

$$p^{N=3}(u) = \sqrt{\frac{2}{\pi}}[1+\tau(\tfrac{1}{3}u^4+\tfrac{3}{2}u^2-\tfrac{7}{16})]e^{-2u^2}+O(\tau^2); \tag{18}$$

and for the polynomials of fourth and higher order,

$$p^{N\geqslant 4}(u) = \sqrt{\frac{2}{\pi}}[1+\tau(-u^4+\tfrac{7}{2}u^2-\tfrac{11}{16})]e^{-2u^2}+O(\tau^{k/2}), \tag{19}$$

where $k=3$ for $N=4$ and $k=4$ for $N\geqslant 5$. For $N\geqslant 4$ there are differences in the higher-order terms only, which explains the results of Fig. 3. In the limit $\tau\to 0$ the invariant density $p(u)$ approaches the Gaussian (3) for all $T_N(x), N=2,3,\dots$ The first correction to the Gaussian is of order $\sqrt{\tau}$ for $T_2(x)$ and of order τ for $N\geqslant 3$. The correction of order $\sqrt{\tau}$ multiplying the Gaussian for $N=2$ is an odd function of u. On the other hand, all corrections of order τ are even functions, which explains the symmetry of the distributions shown in Figs. 2 and 3. In Figs. 11–13 we compare the analytical results with the numerical results from Sec. II. Apparently the agreement is very good.

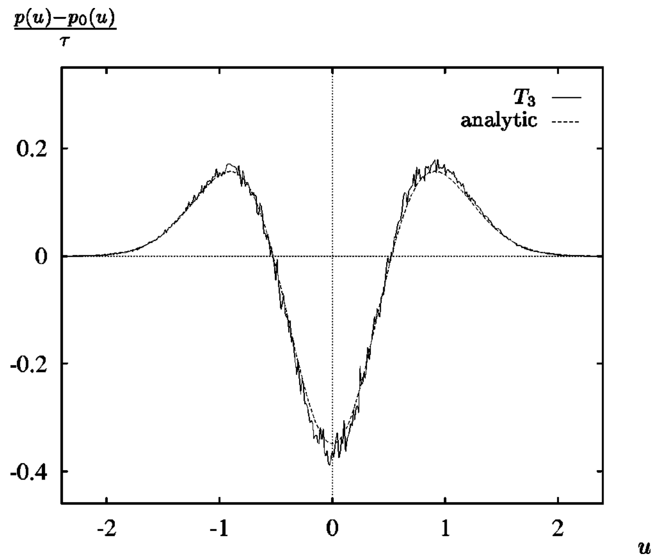

FIG. 12. Comparison of perturbative result (18) with the numerical result for T_3; $\tau=0.1$.

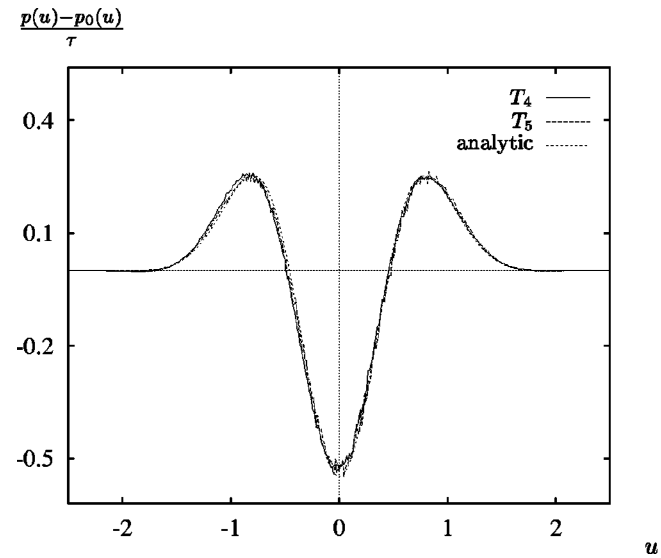

FIG. 13. Comparison of perturbative result (19) with the numerical result for T_4 and T_5; $\tau=0.1$.

IV. RENORMALIZATION GROUP APPROACH

Our analytical results have been obtained for Tchebyscheff maps, but the numerical results of Sec. II show that they seem to have universal significance for larger classes of maps. To explain universal behavior, a common tool is a renormalization group formulation. Let us here be led by the analogy with the Feigenbaum fixed point function $g(x)$ well known from the period doubling scenario [46,47]. This function g is a fixed point of the doubling operator R, defined by

$$Rf(x)=\alpha f\left(f\left(\frac{x}{\alpha}\right)\right), \tag{20}$$

where α denotes the Feigenbaum constant. Universality of α and g can be explained by the fact that at the critical point of period doubling accumulation entire classes of functions f in a suitable function space converge to the fixed point g under successive iteration and rescaling. The behavior in the vicinity of g is universal, which can be understood by studying the linearized version of R in a small vicinity of g. Under the doubling operation, there is only one unstable direction leading away from the universal fixed point g, described by the universal Feigenbaum constant δ and a corresponding universal eigenfunction h of the linearized version of the doubling operator.

In our case the situation is different, but many analogies to the Feigenbaum case hold. We are dealing with probability densities, so we have to look at operators acting in spaces of probability densities. The analogue of the doubling operation is an operation where the time scale parameter τ is increased to twice that value, i.e.,

$$\tau\rightarrow\tau'=2\tau. \tag{21}$$

We then look at the effect this operation has on the invariant density. In the space of probability densities, the Gaussian distribution (obtained for $\tau\rightarrow 0$) is a fixed point under the above time scale transformation. The central limit theorem holds in the limit $\tau\rightarrow 0$; it does not matter if we look at a sequence $\tau_i\rightarrow 0$ or a sequence $2\tau_i\rightarrow 0$. The Perron Frobenius operator has been shown to reduce to the time-scale-independent Fokker-Planck operator for $\tau\rightarrow 0$ [24]. Note that the Gaussian distribution is universal, meaning that many different maps satisfy a central limit theorem; details of the map are unimportant. Hence the Gaussian probability density $p_0(u)$ corresponds to the fixed point function g in the analogy with the Feigenbaum scenario.

The behavior in a small vicinity of the Gaussian fixed point also turns out to be universal, as we find in this paper. This is similar to the universality of δ and h. The first-order correction to the Gaussian density can be understood by studying the ''linearized'' version of the Perron Frobenius operator in a small vicinity of the Gaussian fixed point for small but finite τ [24]. Under time-scale-doubling transformation (21), there appear to be only a few routes leading away from the Gaussian fixed point. If there is scaling behavior with $\tau^{1/2}$, the doubling operation leads to an increase of distance by the factor $2^{1/2}$ and we only find one universal function (in leading order) which describes the deviation from the Gaussian fixed point given by Eq. (10). Our conjecture on universality is thus a conjecture on the spectrum of the linearized version of the Perron Frobenius operator. If there is scaling with τ, the distance doubles under operation (21) and we have evidence for (at least) three different ways how we can leave the Gaussian fixed point under time scale doubling. Hence, more universality classes exist in this case.

V. CONCLUSION

We have investigated the effects that an underlying deterministic chaotic dynamics has on the stationary probability density of a typical Brownian motionlike problem. We consider the motion of a particle in a damping medium under the influence of deterministic chaotic kicks on a fast time scale τ. Decreasing the time scale parameter τ, our dynamical process converges to a Gaussian Markov process, the Ornstein-Uhlenbeck process. We have presented numerical evidence that the route by which this Gaussian process is approached is universal for certain classes of mappings, namely, those where the first-order correction scales with $\sqrt{\tau}$. Up to a nonuniversal factor, we always observe the same functional dependence describing the deviation from the Gaussian distribution for a small but finite time scale parameter. It should be clear that any physical system possesses such a finite time scale, since the Gaussian white noise of a Langevin equation is just an idealization. We have sketched a renormalization group approach to the problem. Similar asymmetric deviations from a Gaussian as in Eq. (17) have also been observed experimentally for velocity differences measured in fully developed turbulent flows; see [25,27] for a detailed comparison with experiments and a suitable chaotic cascade model for these types of problems. Generally, our results are of interest for all those Langevin problems in physics where the Gaussian white noise is thought to be the result of an underlying deterministic dynamics.

---

[1] D. Ruelle and Ya. G. Sinai, Physica A **140**, 1 (1986).
[2] H. Spohn, Rev. Mod. Phys. **52**, 569 (1980).
[3] L. A. Bunimovich and Ya. G. Sinai, Commun. Math. Phys. **78**, 479 (1981).
[4] D. Dürr, S. Goldstein, and J. L. Lebowitz, Commun. Math. Phys. **78**, 507 (1981).
[5] D. Dürr, S. Goldstein, and J. L. Lebowitz, J. Stat. Phys. **30**, 519 (1983).
[6] M. C. Mackey, *Time's Arrow: The Origins of Thermodynamic Behavior* (Springer, New York, 1992).
[7] P. Gaspard, M. E. Briggs, M. K. Francis, J. V. Sengers, R. W. Gammon, J. R. Dorfman, and R. V. Calabrese, Nature (London) **394**, 865 (1998).
[8] T. Tel, J. Vollmer, and W. Breymann, Europhys. Lett. **35**, 659 (1996).
[9] H. van Beijeren, A. Latz, and J. R. Dorfman, Phys. Rev. E **57**, 4077 (1998).
[10] A. K. Evans and P. V. Coveney, J. Phys. A **31**, 5887 (1998).
[11] J. R. Dorfman, Phys. Rep. **301**, 151 (1998).
[12] C. Beck, Physica A **233**, 419 (1996).
[13] C. Beck and G. Roepstorff, Physica A **145**, 1 (1987).
[14] R. V. Jensen and C. R. Oberman, Phys. Rev. Lett. **46**, 1547 (1981).
[15] D. Mayer and G. Roepstorff, J. Stat. Phys. **31**, 309 (1983).
[16] C. Beck, Physica A **169**, 324 (1990).
[17] S. Siboni, Nonlinearity **7**, 1133 (1994).
[18] C. Beck, Commun. Math. Phys. **130**, 51 (1990).
[19] C. Beck, Nonlinearity **4**, 1131 (1991).
[20] C. Beck, G. Roepstorff, and C. Schroer, Physica D **72**, 211 (1994).
[21] R. Badii, G. Broggi, B. Derighetti, M. Ravani, S. Ciliberto, A. Politi, and M. A. Rubio, Phys. Rev. Lett. **60**, 979 (1988).
[22] T. Shimizu, Physica A **164**, 123 (1990).
[23] J. L. Kaplan and J. A. Yorke, *Functional Differential Equations and the Approximation of Fixed Points*, Lecture Notes in Mathematics Vol. 730 (Springer, Berlin, 1979), p. 228.
[24] C. Beck, J. Stat. Phys. **79**, 875 (1995).
[25] C. Beck, Phys. Rev. E **49**, 3641 (1994).
[26] A. Hilgers and C. Beck, Int. J. Bifurcation Chaos Appl. Sci. Eng. **7**, 1855 (1997).
[27] A. Hilgers and C. Beck, Europhys. Lett. **45**, 552 (1999).
[28] C. Beck, Nonlinearity **8**, 423 (1995).
[29] C. Beck, Phys. Lett. A **248**, 386 (1998).
[30] P. Billingsley, *Convergence of Probability Measures* (Wiley, New York, 1968).
[31] N. I. Chernov, Probab. Theory Relat. Fields **101**, 321 (1995).
[32] F. Hofbauer and G. Keller, Math. Z. **180**, 119 (1982).
[33] H. Ishitani, Hiroshima Math. J. **16**, 161 (1986).
[34] M. Jabłoński and J. Malczak, Tohoku Math. J. **35**, 173 (1983).
[35] M. Kac, Ann. Math. **47**, 33 (1946).
[36] G. Keller, C. R. Acad. Sci. URSS **291**, 155 (1980).
[37] S. Wong, Ann. Prob. **7**, 500 (1979).
[38] M. Denker and W. Philipp, Ergod. Theory Dyn. Syst. **4**, 541 (1984).
[39] R. Burton and M. Denker, Trans. Am. Soc. Civ. Eng. **302**, 715 (1987).
[40] I. A. Ibragimov, Theor. Probab. Appl. **7**, 349 (1962).
[41] G. Keller, Z. Wahrscheinlichkeitstheor. Verwandte Geb. **69**, 461 (1985).
[42] M. Ratner, Israel J. Math. **16**, 181 (1973).
[43] Ya. G. Sinai, Soviet Math. Dokl. **1**, 983 (1960).
[44] L. A. Bunimovich, Theor. Probab. Appl. **19**, 65 (1974).
[45] N. G. van Kampen, *Stochastic Processes in Physics and Chemistry* (North-Holland, Amsterdam, 1981).
[46] M. J. Feigenbaum, J. Stat. Phys. **19**, 25 (1978).
[47] C. Beck and F. Schlögl, *Thermodynamics of Chaotic Systems* (Cambridge University Press, Cambridge, 1993).